

# Synergistic Combination of Crystallization and Addition of a Toughening Agent to Promote Recycled Poly(ethylene terephthalate) Performances

Zahir Rahem<sup>a,\*</sup>, Abdelmalek Douibi<sup>a</sup>, Abdelaziz Lallam<sup>b</sup>, Christelle Delaite<sup>c</sup>, and Melia Guessoum<sup>d</sup>

<sup>a</sup> *Laboratoire des Matériaux Polymériques Multiphasiques (LMPMP), Département de Génie des Procédés, Faculté de Technologie, Université Ferhat ABBAS Sétif-1, Sétif, 19000 Algeria*

<sup>b</sup> *Laboratoire de Physique et Mécanique Textiles (LPMT), 11 rue Alfred Werner, Mulhouse, 68093 France*

<sup>c</sup> *Laboratoire de Photochimie et d'Ingénierie Macromoléculaires (LPIM), Institut Jean-Baptiste Donnet, 3b, rue Alfred Werner, Mulhouse, 68093 France*

<sup>d</sup> *Laboratoire de Physico-Chimie des Hauts Polymères (LPCHP), Département de Génie des Procédés, Faculté de Technologie, Université Ferhat ABBAS Sétif-1, Sétif, 19000 Algeria*

\* e-mail: zahir\_rahem@yahoo.fr

Received November 15, 2018; revised February 14, 2019; accepted March 27, 2019

**Abstract**—In order to limit the hydrolytic degradation, recycled polyethylene terephthalate (rPET) was subjected to a heat treatment (annealing) to obtain treated rPET (trPET). To improve the mechanical properties of the latter, it was melt mixed with maleic anhydride grafted styrene ethylene/butylene–styrene copolymer (SEBS-*g*-MA) which acts as a toughening agent then compared to rPET and virgin PET (vPET). The addition of 20% of SEBS-*g*-MA revealed a significant increase in the impact strength by 356, 158, and 188% for trPET, rPET and vPET, respectively. This could be explained by the interface reinforcement resulting from the reaction between the functional groups of the trPET and those of the toughening agent, as identified by Fourier transform infrared analysis. On the other hand, the analysis of the thermal properties using differential scanning calorimetry showed that the cold crystallization temperature of the toughened trPET is decreased and its degree of crystallinity varied slightly compared to that of rPET. The dynamic mechanical thermal analysis pointed out that the presence of 20% of SEBS-*g*-MA in trPET led to a higher storage modulus than that of the toughened vPET. Furthermore, the addition of the toughening agent contributed to a significant promotion of trPET thermal stability.

DOI: 10.1134/S0965545X19050158

## INTRODUCTION

Virgin polyethylene terephthalate (vPET) is a low-cost raw material used in the packaging industry, bottles, fibers and films. This is mainly due to its good comprehensive properties such as transparency, chemical and thermal resistance. However, the poor mechanical behavior and low crystallization rate of PET limit notably its further development [1–6]. The use of PET bottles has been increasing year by year, leading to a huge source of wastes which resulted in a serious ecological problem (pollution) [6, 7]. In order to tackle this problem, the PET recycling constitutes a well promising strategy and is encouraged by the environmental policy of many countries [3].

Thermo-mechanical recycling is one of the most used methods for PET recycling because of its lower cost and simplicity [4, 8, 9]. However, the processing steps at the molten state of this polymer generate a great disadvantage caused by the inevitable degradation of the recycled PET (rPET) when exposed to high

temperatures and shear forces, which reduce its molecular weight and viscosity. In this context, Coltelli et al. [10] reported many factors that could favor PET degradation such as operating conditions like the presence of oxygen and metal catalysts which complexation to the carbonyl groups encourages PET chains scission. Moreover, the presence of retained moisture and contaminants in rPET is considered as a potential harmful parameter which favors rPET hydrolytic degradation leading to a drastic decrease in the rheological properties of the recovered polymer [11–15]. Thus, for a relatively safe processing of rPET, the maximum admissible concentration of residual moisture is limited to 0.01% by weight [6]. A recognized way to reduce rPET tendency to capture moisture and improve its stability against hydrolytic degradation consists of carrying out annealing of the recycled polymer scraps [6, 16, 17]. Indeed, annealing is a heat treatment during which the amorphous parts of

the polymer tend to crystallize inducing a noticeable decrease in their aptitude to recover moisture [6].

Furthermore, the mechanical properties of the rPET resin could also be improved when an elastomer, acting as a toughening agent, is added. This technique is reported in many researches which describe the use of toughening agents to promote rPET performances to get a competitive resin and thus enlarge the use of the recycled polymer [3, 4, 16, 18]. In this context, the dispersion of toughening agents has proved its efficiency in the increase of rPET strength and elongation at break and in the decrease of its Young's modulus [19, 20]. Moreover, in order to enhance the interactions and reduce the interfacial tension between rPET matrix and the elastomers, the use of grafting elastomers with functional groups such as maleic anhydride (MA) and glycidyl methacrylate (GMA) has been found to be an effective method [21–25]. Tan et al. [2] studied the effects of an epoxy macromolecular chain extender and polymethyl methacrylate-*co*-glycidyl methacrylate (PMMA-*co*-GMA) as a compatibilizer between mixtures of PET and ethylene-propylene-diene monomer (EPDM)-*graft*-GMA (EPDM-*g*-GMA) and they concluded a noticeable increase in the torque due to the reaction of the epoxy groups with the hydroxyl and carbonyl end groups of PET. Raiisi-Nia et al. [4] studied the effects of glycidyl methacrylate grafted acrylonitrile-butadiene rubber (NBR-GMA) on the performances of rPET and found that relatively to the blend rPET/NBR, the rubber phase is more finely dispersed into the PET matrix which improves significantly the impact strength. Similarly, maleic anhydride grafted polyethylene-octene elastomer copolymer (POE-*g*-MA) [19], styrene-ethylene/butylene-styrene (SEBS-*g*-MA) [25, 26], ethylene-*co*-propylene rubber (EPR-*g*-MA) [27, 28], acrylonitrile-butadiene-styrene (ABS-*g*-MA) [24] and natural rubber (NR) [29] were respectively incorporated to PET as toughening agents. It has been noticed that functional groups of the toughening agents react with PET carboxyl and/or hydroxyl end groups to form copolymer at the interface which reinforces significantly the resin [3, 23, 25]. The effectiveness of SEBS grafted copolymers in promoting PET blends performances has already been stated by Colteli et al. [30, 31] when studying the properties of PET/low density polyethylene (LDPE) mixtures melt blended in presence of transesterification catalysts. The studied PET/LDPE blends were found to show a cocontinuous morphology in presence of SEBS grafted with diethyl maleate (DEM) (SEBS-*g*-DEM) due to its lower viscosity which allows its migration in the blend interfacial region and the covering of the LDPE phase [30]. Also, the viscosimetry and size exclusion chromatography measurements confirmed the increase in PET molecular weight due to the grafting of PET to SEBS chains [31].

In order to improve the hydrolytic stability and the mechanical properties of rPET with respect to vPET,

our study has been focused primary on the annealing treatment to convert rPET to a more crystallized material (trPET) then the latter is combined with the toughening agent SEBS-*g*-MA. To the best of our knowledge, no study has tried to blend trPET with a toughening agent. Furthermore, it has been proven that the reduction of the moisture content is the key tool to reduce chain scissions and enhance the mechanical resistance of rPET. This could be achieved if rPET scraps are first annealed to drive away the inner moisture confined into its amorphous phase before incorporating the toughening agent.

## EXPERIMENTAL

### *Materials*

vPET was supplied by China Resources Packaging Materials Co., LTD, China under the trade name CR-8828 (intrinsic viscosity 0.86 dL/g). The used PET wastes were obtained from post-consumer PET bottles. After removing the parts of the bottles containing ink and adhesive, the remaining parts were carefully washed in a 20% sodium hydroxide (NaOH) solution at 80°C. The toughening agent SEBS-*g*-MA, containing 1.84% of maleic anhydride, was supplied by Shell Chemical Co. (USA) under the trade name of Kraton FG 1901X.

### *Processing*

Before processing by melt-mixing with SEBS-*g*-MA, rPET scraps were first heated at 150°C under vacuum for at least 5 h then cooled slowly to ambient temperature to obtain trPET. Then, virgin, recycled and treated PET resins and SEBS-*g*-MA were dried at 100°C for 24 h and at 60°C for 6h, respectively. Then, formulations of vPET, rPET and trPET with 10 and 20% by volume of SEBS-*g*-MA were melt-mixed in a Brabender plastograph at a temperature of 260°C and a mixing speed of 45 rpm for a period of 8 min. After pelletizing, the formulated granules are dried before the elaboration of films and samples for further characterizations.

### *Characterization Techniques*

**Mechanical properties.** Tensile and impact tests specimens were prepared using a Carver molding machine at a temperature of 260°C and for a period of 8 min. Tensile properties were evaluated on a MTS-20/M apparatus using a cross-head speed of 5 mm/min. Charpy impact strength was determined using a Ceast impact machine equipped with a hammer 1.8 kg delivering an impact energy 7.5 kJ.

**Scanning electron microscopy (SEM).** The morphologies of trPET/SEBS-*g*-MA formulations were observed by Scanning Electron Microscopy (SEM) carried out on a S-2360N instrument. The cryo-frac-

tured surfaces of the specimens were coated with gold before observation.

**Fourier transform infrared spectroscopy (FTIR).** FTIR analysis was used to detect interactions at the interface trPET/SEBS-g-MA and spectra were recorded in transmission from 400 to 4000  $\text{cm}^{-1}$  with a Perkin Elmer FTIR Spectrum 1000 spectrophotometer.

**Differential scanning calorimetry (DSC).** DSC was conducted on a TA differential scanning calorimeter (DSC Q200). The samples were heated from 25 to 280°C, kept at this temperature for a period of 3 min, then cooled to 25°C, kept at this last temperature for 3 min, and finally heated to 280°C. The heating and cooling rates were 10 grad/min. The degrees of crystallinity ( $\chi_c$ ) and ( $\chi_{cc}$ ) were evaluated according to the following equation:

$$\chi_c = \frac{\Delta H}{\Delta H_m^0 \omega_{\text{PET}}} \times 100. \quad (1)$$

For the cooling curves,  $\Delta H = \Delta H_c$  is the crystallization enthalpy of the sample. Whereas for the second heating thermograms,  $\Delta H = \Delta H_m$  is the melting enthalpy of the sample.  $\omega_{\text{PET}}$  represents the volume fraction of PET into the studied composition. The considered melting enthalpy of a 100% crystalline PET ( $\Delta H_m^0$ ) was 140 J/g [6].

**Dynamic mechanical analysis (DMA).** Measurements were carried out with a dynamic mechanical analyzer (Rheoplus MCR), on rectangular samples presenting the dimensions (40 × 10 × 2)  $\text{mm}^3$ . DMA spectra were recorded in shearing mode by heating the samples to 150°C at a heating rate of 3 deg/min. The samples were scanned at a fixed frequency of 1 Hz with a dynamic strain of 0.1%.

**Isothermal gravimetric analysis (ITGA).** ITGA was carried out to measure the weight loss of the samples as an indicator of their thermal stability during processing. The measurements were performed using a Q500 thermo-gravimetric analyzer at 260°C and for a period of 30 min under oxygen gas atmosphere.

## RESULTS AND DISCUSSION

### *DSC Analysis of rPET and trPET*

Figure 1 depicts the DSC thermograms related to the first heating runs of rPET and trPET. After the glass transition temperature  $T_g$ , the rPET thermogram shows a small exothermic peak, observed between 90 and 130°C, which corresponds to the crystallization of amorphous regions (Fig. 2). This exotherm is due to the chains tendency to rearrange into crystals during heating. However, the crystallization exotherm peak is not detected in the trPET thermogram. This can be explained by the fact that the crystallization was already carried out during the annealing of rPET. The crystallinity degree increases slightly from 30.1% for

rPET to a value of 34.5% after annealing. On the other hand, the melting behavior of rPET is shown by the endotherm observed around 250°C, whereas that of trPET is exhibited by a principal melting peak similar to that observed for rPET and another small endotherm depicted at about 168°C. The existence of two melting peaks in trPET has already been reported by several authors who suggested that when PET is subjected to heat treatment, multiple lamellae populations are present simultaneously which results in a multiple melting behavior [32–34]. Sawatari and Matsuo [35] proposed that PET thermal treatment allows crystallites separation into two phases and showed that the area and the position of these multiple peaks are dependent on the thermal treatment conditions such as temperature and duration. They suggested also that the modifications which may be noticed on the peaks profile could be induced by crystalline defaults and differences in crystallites sizes. Furthermore, the existence of multiple melting peaks is explained by the crystalline morphology distribution in terms of size and perfection. In addition, Avila-Orta et al. [36] reported that multiple peaks are observed due to the melting–recrystallization–melting processes, which suggests that during the heating scan, a fraction of the crystals formed during isothermal crystallization melts at a low temperature; while recrystallization or reorganization occurs in the remaining fraction which produces crystals with higher perfection that melt at higher temperatures.

### *Crystallization Behavior of vPET and trPET into the Mixtures with SEBS-g-MA*

The DSC thermograms from the cooling and second heating runs for vPET and its mixtures with SEBS-g-MA are represented respectively in Figs. 3a and 3b. The thermograms, given in Fig. 3a, display only the PET cold crystallization peak. For vPET, the cold crystallization temperature  $T_{cc}$ , taken at the maximum of this peak, is detected at 206°C. When vPET is mixed with SEBS-g-MA, the cold crystallization peak is displaced towards higher temperatures and is observed around 215°C for both mixtures containing 10 and 20% of the toughening agent. This indicates that during cooling, the SEBS-g-MA acts as a plasticizer and favors the rearrangements of vPET chains which allow them to crystallize from higher temperatures. This observation supports also the fact that in presence of the toughening agent, the crystallization rate increases because the degree of supercooling required for the crystallization is reduced. Consequently, the crystallization peak narrows and the vPET crystallinity into the mixtures increases, as it is reported in Table 1.

On the other hand, Fig. 3b depicts the heating thermograms of vPET and vPET/SEBS-g-MA mixtures. An important increase is noticed on the crystallinity due to the plasticizing effect of the toughening agent

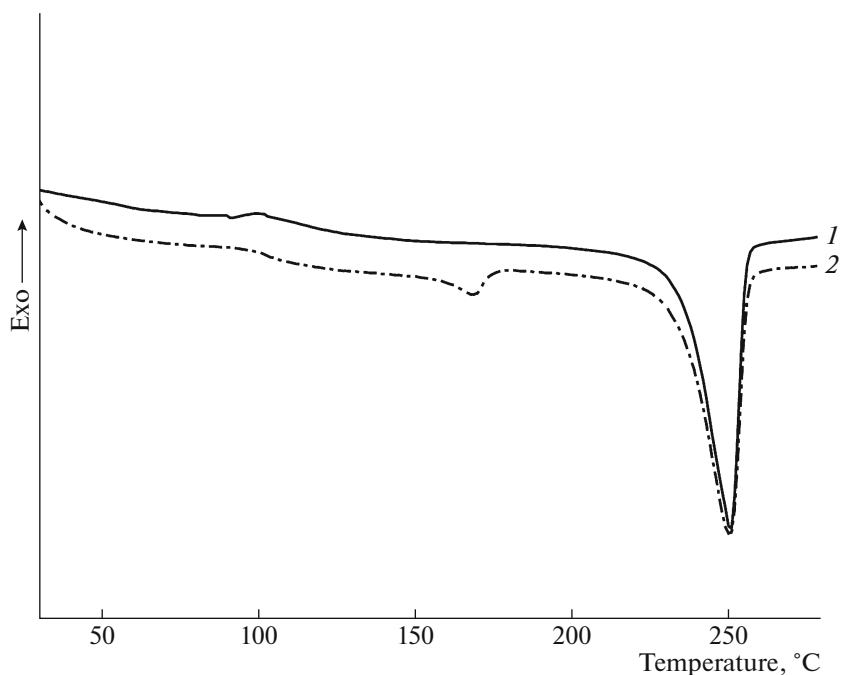


Fig. 1. First heating DSC thermograms of (1) rPET and (2) trPET.

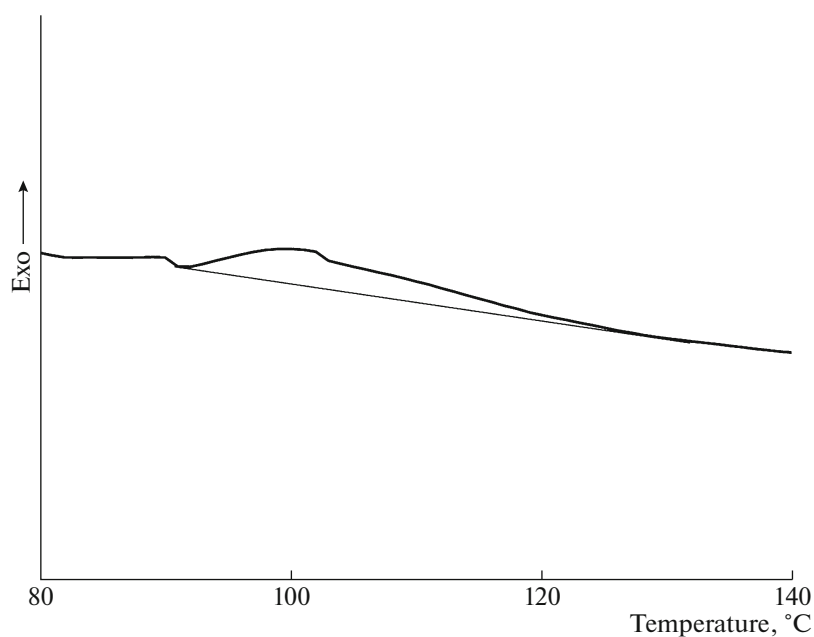
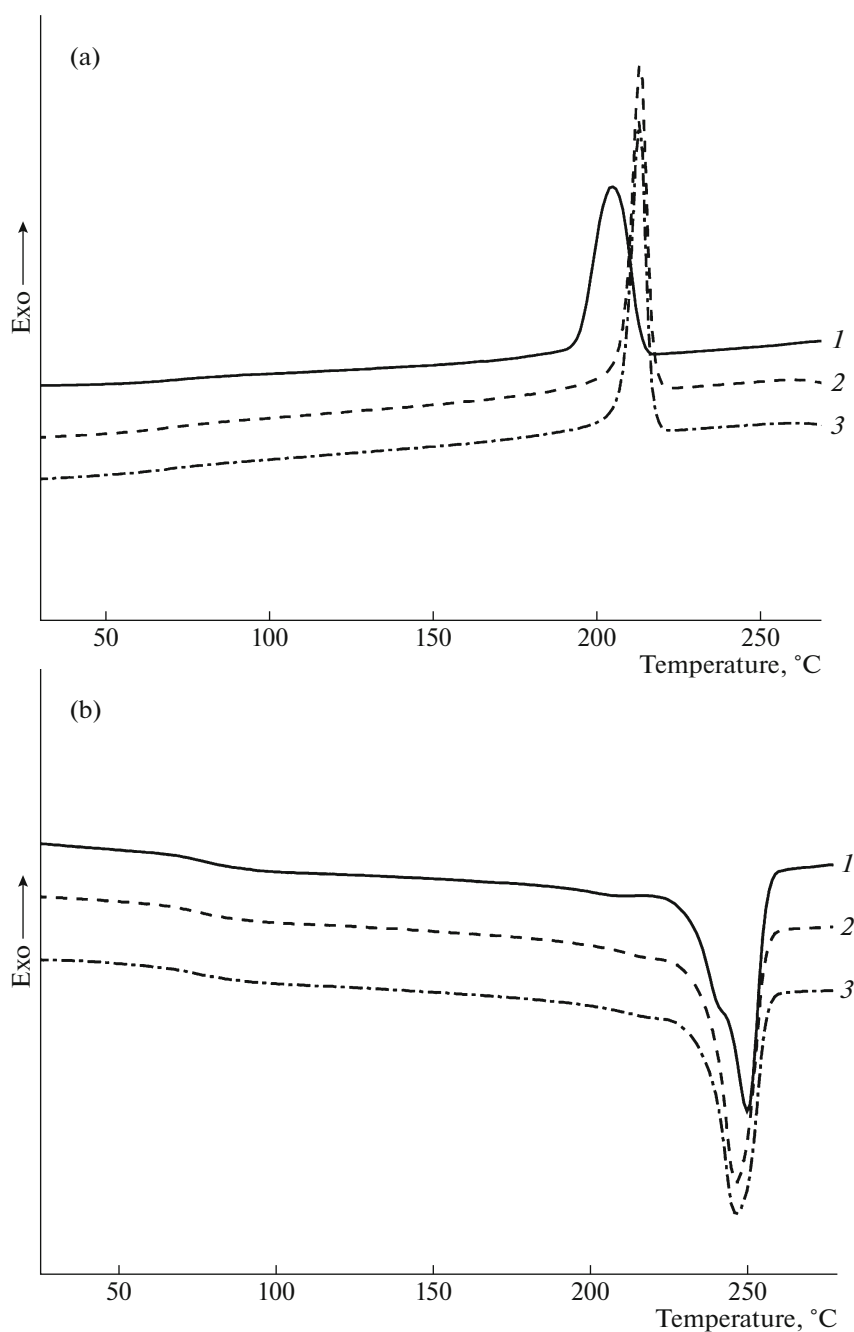


Fig. 2. Crystallization pic of rPET during the first heating DSC thermograms.

which favors the mobility of the polymer chains and promotes the development of crystallites. However, the melting peak temperatures  $T_m$  of the mixtures are slightly decreased with respect to vPET. This can be explained by the fact that the addition of the toughening agent reduces also the size and the perfection degree of the formed PET crystals resulting in the decrease of their stability.

Moreover, Figs. 4a and 4b represent, respectively, the DSC thermograms of the cooling and second heating runs of trPET and trPET/SEBS-*g*-MA mixtures with 10 and 20% of SEBS-*g*-MA. The cooling thermograms (Fig. 4a) show that, trPET exhibits a noticeably higher cold crystallization temperature  $T_{cc}$  at around 213°C. This high value is explained by the fact that trPET may include short chains that appear



**Fig. 3.** DSC thermograms of (1) vPET, (2) vPET/SEBS-*g*-MA 10%, (3) vPET/SEBS-*g*-MA 20%: (a) cooling runs, (b) second heating runs.

more amenable to reorganization and crystallization compared to longer vPET chains. Furthermore, it is observed that when SEBS-*g*-MA is added, the trPET phase crystallizes for lower temperatures compared to trPET alone, which means that a higher undercooling of the melt is necessary for the crystallization to occur. This behavior is essentially explained by the strong effect of the chemical interactions on chain dynamics. Indeed, the crystallization of trPET is slowed down as a result of the lower chains mobility resulting from the

interactions between the hydroxyl groups of trPET and the anhydride groups of SEBS-*g*-MA. Consequently, the crystallinity varies slightly compared to the vPET and its mixtures (Table 1).

Similarly, the heating thermograms of trPET and trPET/SEBS-*g*-MA do not show noticeable variations of the crystallinity and melting temperature of trPET into the mixtures. This is due to the strong restrictions imposed by the interactions with the toughening agent on the chains mobility. Thus, it seems that in the case

**Table 1.** DSC thermograms analysis for vPET, trPET and their mixtures with SEBS-*g*-MA

Sample	$T_m$ , °C	$\Delta H_m$ , J/g	$\chi_c$ , %	$T_{cc}$ , °C	$\Delta H_{cc}$ , J/g	$\chi_{cc}$ , %
vPET	251	59	42	203	49	35
vPET/SEBS- <i>g</i> -MA 10%	248	60	48	215	50	40
vPET/SEBS- <i>g</i> -MA 20%	248	56	50	215	46	41
trPET	250	67	48	213	56	40
trPET/SEBS- <i>g</i> -MA 10%	251	60	48	212	52	43
trPET/SEBS- <i>g</i> -MA 20%	250	54	48	209	49	43

of the virgin resin mixtures, the plasticizing effect of the toughening agent prevails over the interactions involved between the two materials and promotes the crystallization process. In opposite, in trPET mixtures, the interactions developed at the interface with the toughening agent predominate and hinder notably the polymer crystallinity. Also, the presence of multiple melting peaks is attributed to the presence of two types of crystalline morphology: folded-chain and partially extended chain crystals.

*Mechanical Properties of trPET, vPET  
and rPET Mixtures with SEBS-*g*-MA*

The Charpy impact strength values of vPET, trPET and rPET and their mixtures with SEBS-*g*-MA are represented in Fig. 5. The vPET presents an impact resistance which is around 10 kJ/m<sup>2</sup>, whereas trPET exhibits a relatively brittle behavior, with a resilience approximating a value of 6 kJ/m<sup>2</sup>, resulting from the eventual molecular mass decrease during its recycling. The impact strength of rPET is about 3.8 kJ/m<sup>2</sup> due also to the hydrolytic degradation during the processing steps at the molten state. The addition of 10% of SEBS-*g*-MA to trPET results in an impressive jump in the Charpy impact energy reaching that of vPET (with 0% of SEBS-*g*-MA). Indeed, the reinforcing effect of the toughening agent is more noticeable because it is observed that when 20% of SEBS-*g*-MA is added to trPET, the impact strength value is improved by more than 356%, which indicates that a brittle to ductile transition occurs. This supposes that the higher the anhydride groups concentration of SEBS-*g*-MA the more the reaction with hydroxyl groups of trPET and the better the interfacial adhesion. On the other hand, the addition of 20% of SEBS-*g*-MA to both trPET and vPET results almost in a same impact strength value (28 kJ/m<sup>2</sup>). This can be explained by a better interfacial adhesion that effectively compensates the negative effects generated by the recycling of PET. On the contrary, the slight increase in the impact strength (10.1 kJ/m<sup>2</sup>) with the addition of 20% of SEBS-*g*-MA to rPET, reaching that of vPET and trPET (with 0 and 10% of SEBS-*g*-MA, respectively), can be related to

the negative effect of the hydrolytic degradation of the rPET blends. This proves that the heat treatment (annealing) limits the hydrolytic degradation of rPET. As a comparison of our results with those of Zhang et al. [25], the later found that the addition of 15% (by weight) of SEBS-*g*-MA to rPET (initially, the impact strength was 4 kJ/m<sup>2</sup>) resulted in an increase to 11.5 kJ/m<sup>2</sup>. In our case, the addition of a slightly lower concentration of SEBS-*g*-MA (13.9% by weight, after conversion) to trPET (initially, the impact strength was 6 kJ/m<sup>2</sup>), yields a higher value (28 kJ/m<sup>2</sup>) for this property. This highlights the importance of rPET crystallization in our study, and emphasizes the synergistic effect brought by its combination to the reinforcing effect of the toughening agent.

The tensile properties of vPET, rPET and trPET and their mixtures reinforced with 10 and 20% of SEBS-*g*-MA are determined and reported in Figs. 6 and 7. vPET and trPET are brittle materials as it is evidenced from their low elongation at break (3.1 and 1.58%, respectively) and the absence of the yield point on their stress-strain curves. The addition of SEBS-*g*-MA leads to a significant improvement of their elongation at break and tensile strength resulting in more tough and strong materials (Fig. 6). These results are in agreement with those obtained in Charpy impact strength measurements.

As expected, vPET presents higher tensile strength, stress and elongation at break compared to those of trPET (Table 2). This can be explained by the fact that during its reprocessing, trPET exhibits chains scission due to its partial hydrolytic degradation. However, the addition of 20% SEBS-*g*-MA to the trPET results to an overtake of its tensile strength and elongation at break with respect to those of vPET (even mixed to 20% of SEBS-*g*-MA). The enhancement in the elongation at break is due to an efficient stress transfer from the matrix to the elastomeric particles resulting from the interfacial reaction that occurs between the hydroxyl groups of PET and the anhydrides of the functionalized toughening agent; the higher the interfacial adhesion between vPET and trPET matrices and SEBS-*g*-MA particles, the better the mechanical

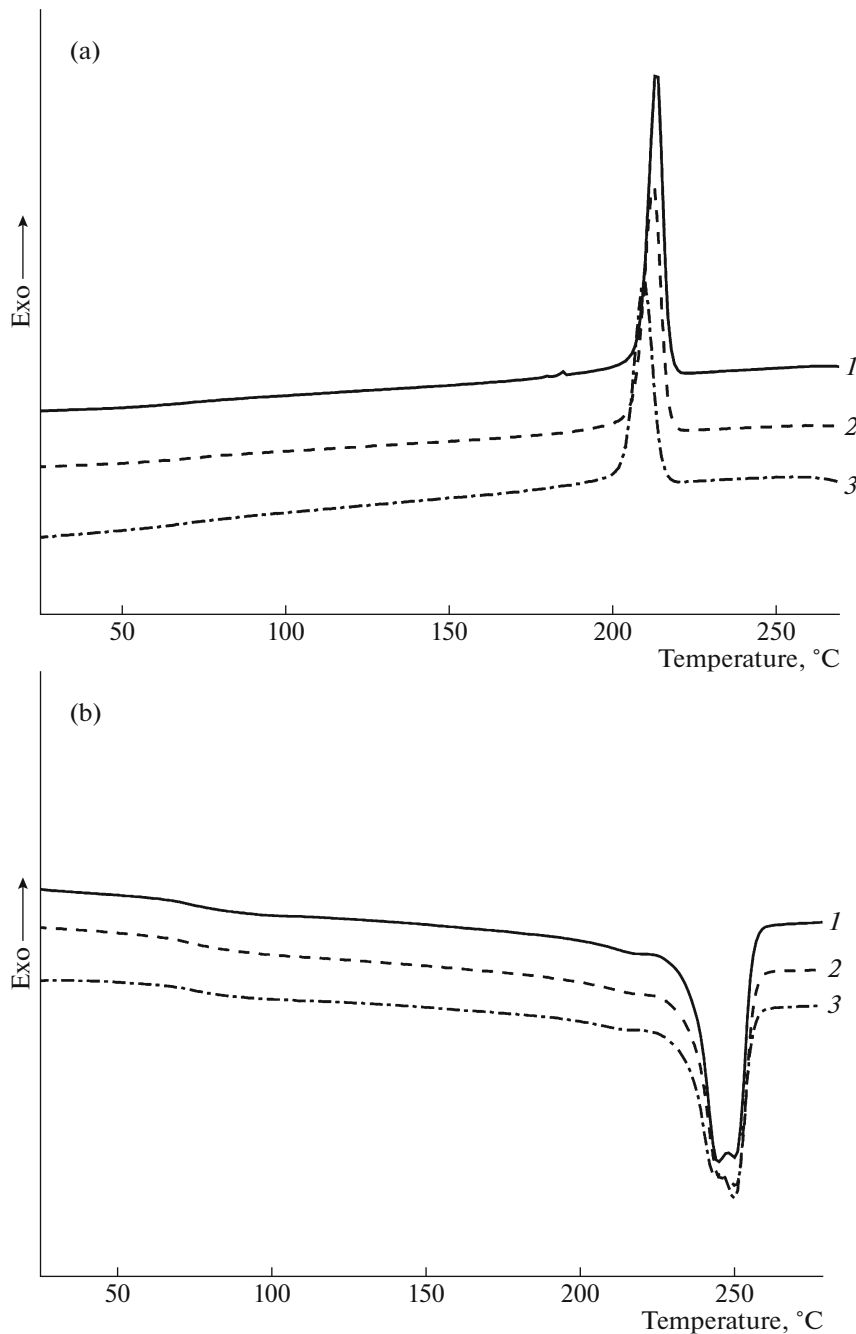


**Fig. 4.** DSC thermograms of (1) trPET, (2) trPET/SEBS-*g*-MA 10%, (3) trPET/SEBS-*g*-MA 20%: (a) cooling runs, (b) second heating runs.

properties of the blends [25]. The decrease in the tensile modulus of vPET and trPET mixtures caused by the addition of the toughening agent was expected due to the low tensile modulus of the later.

The stress-stain curves of trPET and rPET and their mixtures with SEBS-*g*-MA are depicted in Fig. 7. It can be seen that the rPET have a lower elongation at break (1.28 MPa) and higher elastic modulus than that of trPET. This is due to the presence of mois-

ture during processing leading obviously to the hydrolytic degradation of the resin. The slight increase in the elongation at break is clearly observed when 20% of SEBS-*g*-MA was added to rPET. Consequently, the incorporation of SEBS-*g*-MA with a concentration of 20% appears to be particularly advantageous for trPET because it gives a higher reinforcing effect than that obtained when this content of the toughening agent is added to rPET and the virgin resin. It seems also that the crystallization of trPET contributes efficiently to

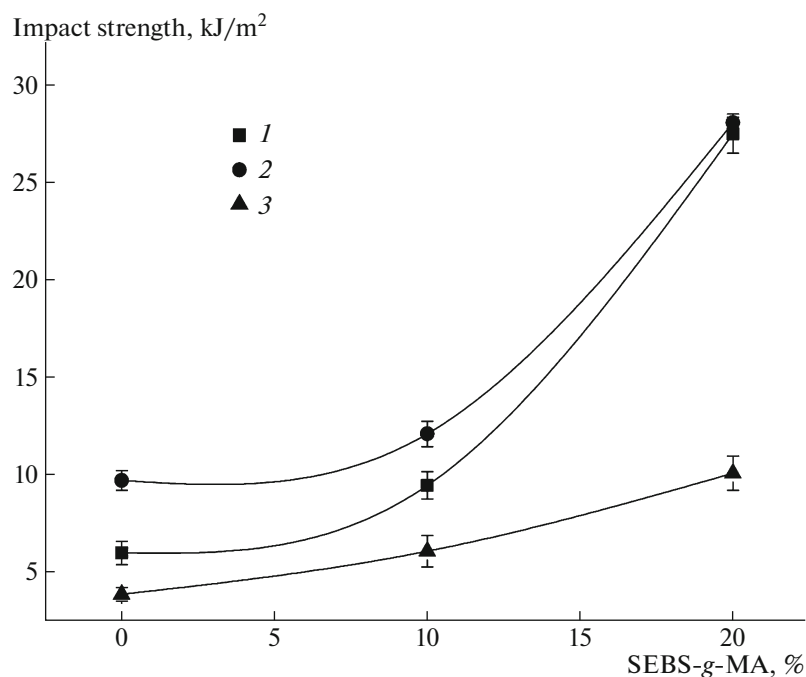


**Fig. 5.** Variations of Charpy impact strength of (1) trPET, (2) vPET, and (3) rPET and their mixtures with SEBS-g-MA versus SEBS-g-MA content.

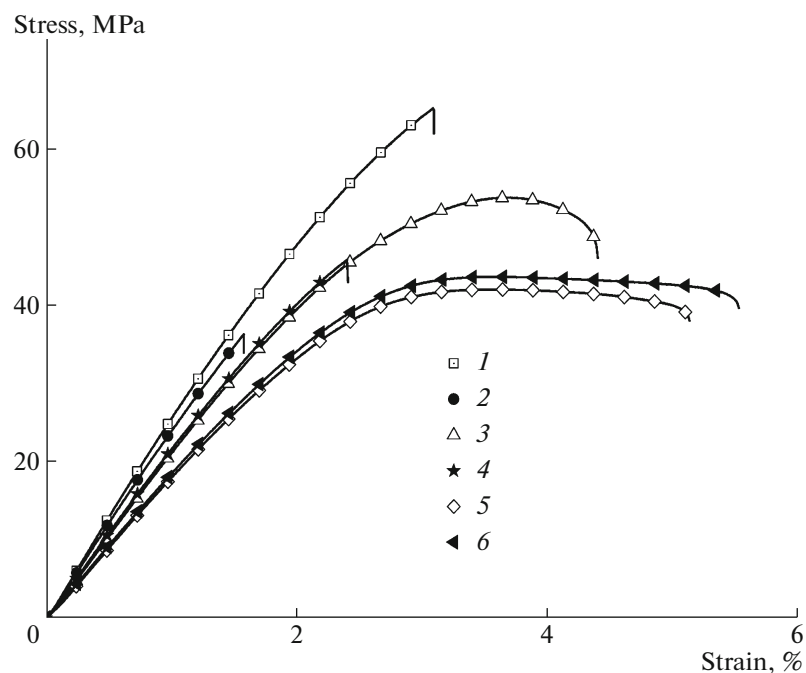


**Fig. 6.** Stress-strain curves of (1) vPET, (2) trPET, and their mixtures with SEBS-g-MA: (3) vPET/SEBS-g-MA 10%, (4) trPET/SEBS-g-MA 10%, (5) vPET/SEBS-g-MA 20%, (6) trPET/SEBS-g-MA 20%.

the reduction of its hydrolytic degradation proceeding by chains scission reactions during the melt mixing. Thus, from the combination of the crystallization process to diminish the trPET aptitude to recover mois-

ture and the rubbery toughening action by the incorporation of the SEBS-g-MA, it is possible to acquire materials with mechanical performances that approach or simply surpass those obtained from vPET.



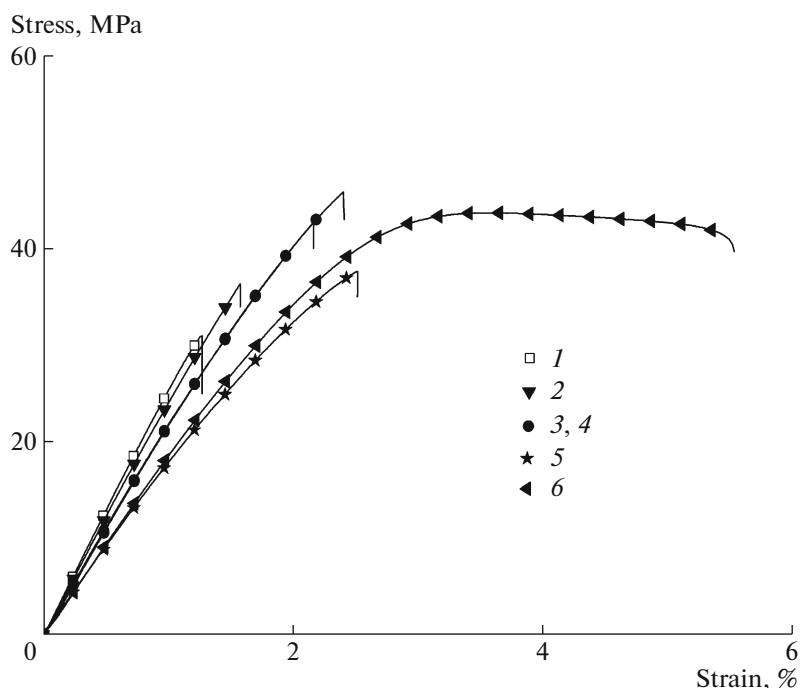


**Fig. 7.** Stress-strain curves of (1) rPET, (2) trPET, and their mixtures with SEBS-*g*-MA: (3) rPET/SEBS-*g*-MA 10%, (4) trPET/SEBS-*g*-MA 10%, (5) rPET/SEBS-*g*-MA 20%, (6) trPET/SEBS-*g*-MA 20%.

#### Fourier Transform Infrared Spectroscopy (FTIR)

In order to get insight into the interfacial region between trPET matrix and the toughening agent, trPET/SEBS-*g*-MA (with 20% of SEBS-*g*-MA) blend has been analyzed by FTIR spectroscopy as it is shown by the obtained spectra given in Fig. 8. The interaction between trPET and SEBS-*g*-MA is obviously demonstrated by the disappearance of the absorbance band characteristic of the carbonyl owing to the maleic anhydride groups, which appears in the FTIR spec-

trum of SEBS-*g*-MA around  $1780\text{ cm}^{-1}$ . This result supports the fact that these groups have totally reacted with hydroxyl end groups of trPET (Fig. 9), as it has been proposed by Kalfoglou et al. [37]. According to this result, the domain size of SEBS-*g*-MA particles into the trPET matrix should be rather reduced due to the significant contribution of the interfacial reaction to the improvement of the dispersion. Indeed, it has been reported that the interaction between the carbonyl groups of the maleic anhydride and the trPET

**Table 2.** Tensile properties of vPET, trPET and rPET melt mixed with SEBS-*g*-MA

Sample	Elastic modulus, GPa	Stress at break, MPa	Tensile strength, MPa	Elongation at break, %
vPET	$2.49 \pm 0.02$	$64.5 \pm 1.7$	$112.4 \pm 9.5$	$3.10 \pm 0.25$
vPET/SEBS- <i>g</i> -MA 10%	$2.07 \pm 0.04$	$54.0 \pm 4.5$	$161.1 \pm 5.6$	$4.40 \pm 0.49$
vPET/SEBS- <i>g</i> -MA 20%	$1.78 \pm 0.04$	$38.3 \pm 1.9$	$161.6 \pm 9.6$	$5.10 \pm 0.61$
trPET	$2.39 \pm 0.11$	$37.2 \pm 4.6$	$29.2 \pm 5.8$	$1.58 \pm 0.3$
trPET/SEBS- <i>g</i> -MA 10%	$2.16 \pm 0.09$	$53.0 \pm 5.9$	$90.1 \pm 9.0$	$2.45 \pm 0.57$
trPET/SEBS- <i>g</i> -MA 20%	$1.81 \pm 0.03$	$41.0 \pm 0.7$	$184.2 \pm 7.8$	$5.50 \pm 0.52$
rPET	$2.59 \pm 0.04$	$30.8 \pm 1.4$	$20.4 \pm 4.2$	$1.28 \pm 0.22$
rPET/SEBS- <i>g</i> -MA 10%	$2.16 \pm 0.05$	$42.3 \pm 1.8$	$35.1 \pm 5.5$	$2.17 \pm 0.36$
rPET/SEBS- <i>g</i> -MA 20%	$1.81 \pm 0.04$	$37.4 \pm 2.8$	$52.7 \pm 3.6$	$2.53 \pm 0.39$

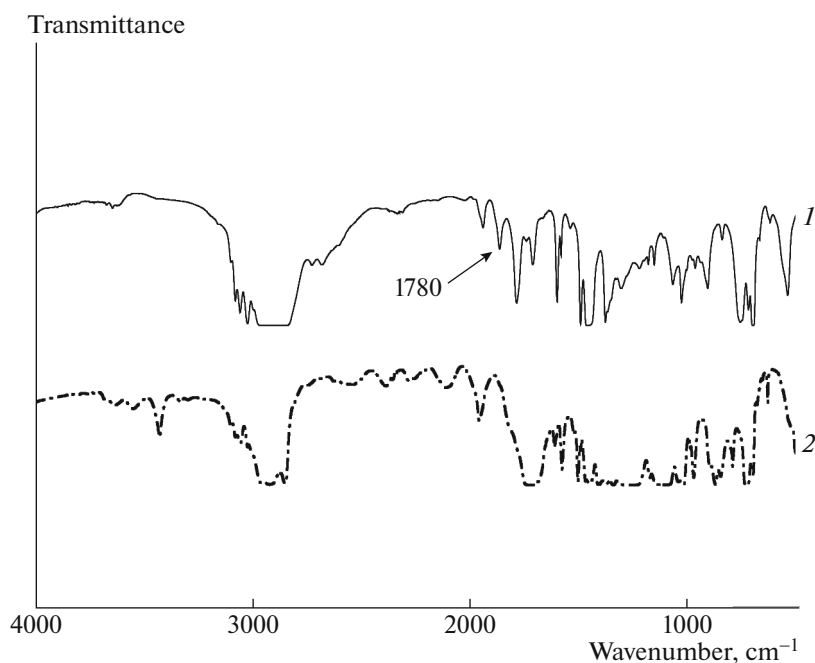


Fig. 8. FTIR spectra of (1) SEBS-*g*-MA and (2) trPET mixed with 20% of SEBS-*g*-MA.

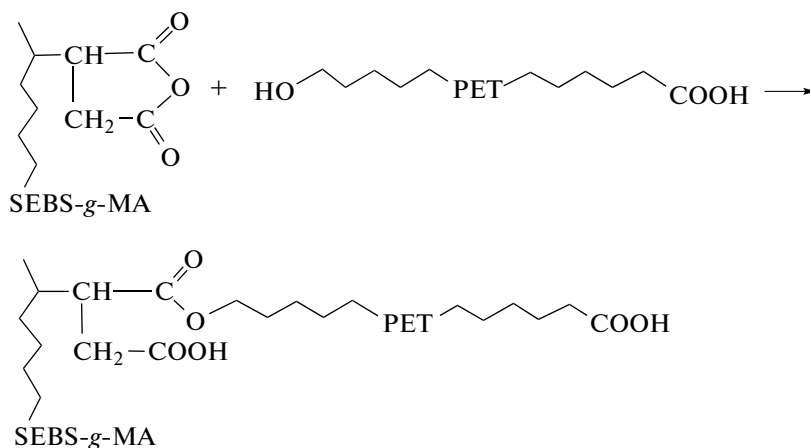


Fig. 9. Interaction between PET and SEBS-*g*-MA. Reprinted with permission from [38], Copyright 2004, John Wiley and Sons.

hydroxyl groups could not only enhance the mechanical properties of the blend but also optimize the interface and decrease the domain size of the dispersed phase [1].

#### *Microstructure Analysis of trPET and trPET/SEBS-*g*-MA Mixtures*

Figures 10a–10c show SEM micrographs taken from the impact fractured surfaces of trPET and trPET melt mixed with 10 and 20% of SEBS-*g*-MA, respectively. The micrograph of the trPET reveals a relatively smooth surface with some coarse fibrils. In

opposite, trPET/SEBS-*g*-MA mixtures exhibit a more extensive deformation taking the appearance of shear bands that cross the whole fracture surface and denoting the transition in the fracture mechanism from crazing to shear yielding [1]. The roughness of the fracture surface associated to the formation of shear bands during the rupture of a toughened sample could be attributed to the crack deflection and creation of additional surface area or new cracks during the material solicitation. These would imply that some of applied energy is consumed by processes implicated into the creation of new fracture surfaces which would result in a higher impact resistance of the material

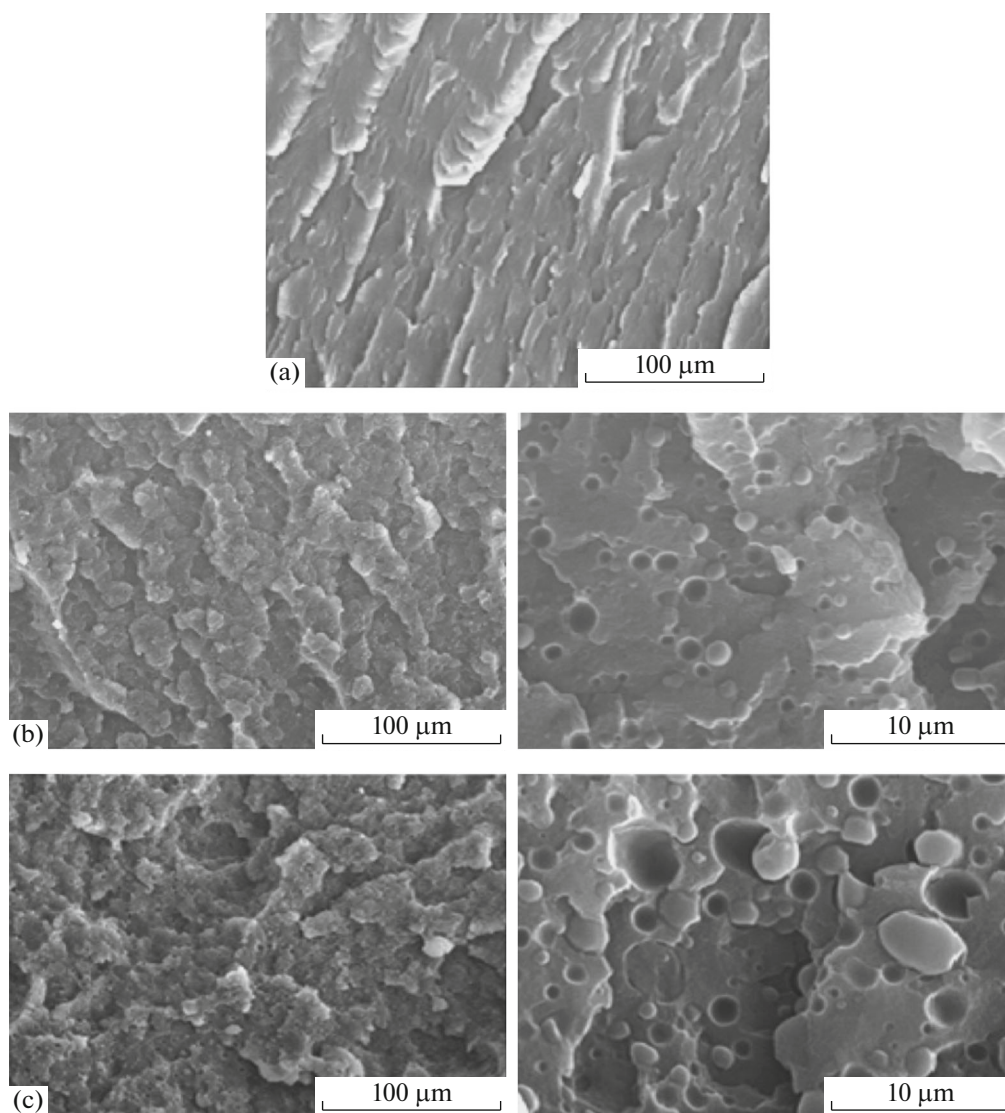


**Fig. 10.** SEM micrographs of (a) trPET and trPET melt mixed with: (b) 10 and (c) 20% of SEBS-*g*-MA.

[39]. SEBS-*g*-MA domains are evidenced as spherical nodules presenting dimensions between 0.8 and 1.5  $\mu\text{m}$  for the formulation with 10% of SEBS-*g*-MA and between 0.7 and 5  $\mu\text{m}$  for that containing 20% of the toughening agent. Similarly, Tan et al. [2] and Park et al. [40] observed spherical domains when reinforcing PET with EPDM-*g*-MA. Moreover, previous studies [1, 39] observed elastomer nodules dispersed into a PET matrix and reported that the domain size is apparently dependent on the toughening agent content, among other parameters. It is worth noting that the two mixtures with 10 and 20% of SEBS-*g*-MA show little evidence of elastomer nodules pulled out and after fracture these domains are still embedded into the trPET matrix. This would not be possible if the adhesion of the toughening agent to the matrix was not sufficiently strong. Indeed, the interfacial reaction allowed the development of strong interactions that

ensures a good wettability of the toughening agent by the trPET matrix. This results in a larger contact surface enabling a better stress transfer that allows the consumption of the applied energy in processes of cavitation and debonding of the SEBS-*g*-MA particles at the interface between the trPET matrix and the elastomer.

#### *Viscoelastic Properties of vPET and trPET Mixed with SEBS-*g*-MA*

Figures 11a, 11b depict, respectively, the variations of the storage modulus  $G'$  and damping factor ( $\tan\delta$ ) for vPET, trPET and their mixtures with 20% of SEBS-*g*-MA as a function of temperature. Figure 11a shows that in the glassy region, vPET and trPET present, respectively, a storage modulus of about 1170 MPa and 1112 MPa, which decreases monotonically with

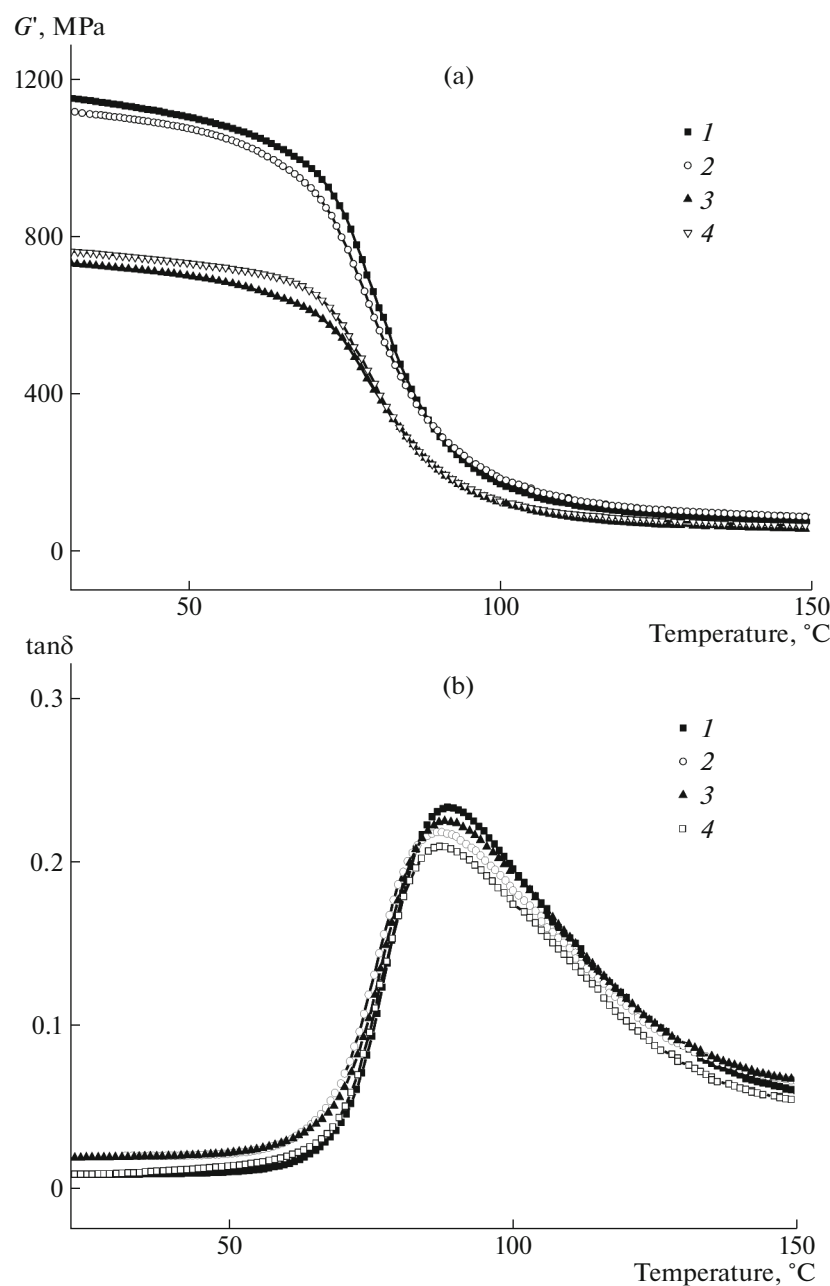


**Fig. 11.** Variations of (a) the storage modulus and (b)  $\tan\delta$  versus temperature for (1) vPET, (2) trPET, and their mixtures with 20% of SEBS-*g*-MA: (3) vPET/SEBS-*g*-MA 20%, (4) trPET/SEBS-*g*-MA 20%.

temperature. As the polymers glass transition temperatures are attained around 89 $^{\circ}\text{C}$  for vPET and 86 $^{\circ}\text{C}$  for trPET, the storage modulus drops suddenly when it approaches the molten state. Consequently, peaks are detected in the variations of  $\tan\delta$  and present their maxima at these temperatures (Fig. 11b). The fact that vPET shows a slightly higher  $T_g$  than that detected for trPET is explained by the possible existence of trPET shorter chains resulting from the polymer chains scissions occurring after the polymer reprocessing.

After the incorporation of 20% of SEBS-*g*-MA, a significant decrease is noted on the mixtures storage modulus which is reduced by about 36 and 32% relatively to those of the vPET and trPET, respectively. These results seem to be in good agreement with the tensile test measurements and are due to the decrease in the material rigidity by the rubbery toughening agent [25]. Similarly to Young's modulus variations, it is observed that trPET/SEBS-*g*-MA blend exhibits a higher storage modulus than that of vPET/SEBS-*g*-MA blend. This implies that the trPET/SEBS-*g*-MA

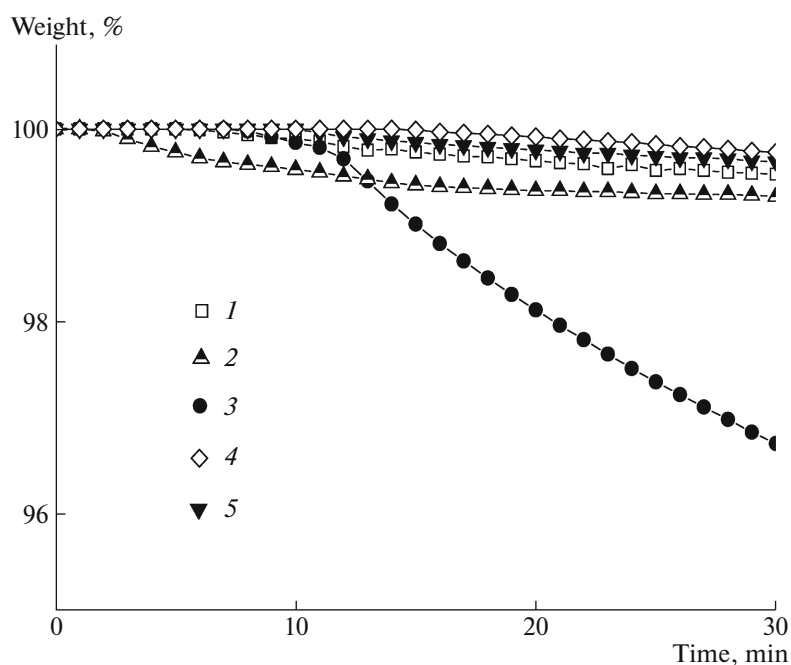


**Fig. 12.** Isothermal thermogravimetric curves of (1) vPET, (2) trPET, (3) SEBS-*g*-MA, (4) vPET/SEBS-*g*-MA 20%, (5) trPET/SEBS-*g*-MA 20%.

blend presents a higher stiffness than that of the mixture based on the virgin resin, which supports the evidence that due to the higher rate of interfacial reactions between the trPET functional groups and the toughening agent, a more rigid interface is obtained.

On the other hand, small variations are noted on the  $T_g$  values of trPET and vPET after melt blending in presence of the toughening agent. This suggests that the expected plasticizing effect of the elastomeric particles competes with the increased interface rigidity and the immobilization of the polymers segments due to their interactions with the toughening agent. The determination of  $T_g$  values from the variations of  $\tan \delta$  suggests that in the case of vPET/SEBS-*g*-MA blend, the plasticizing effect of the toughening agent dominates over the interactions involved with the polymer. In opposite, the decrease in the  $T_g$  of trPET into the blend in comparison with that of the unmodified trPET implies that in the trPET/SEBS-*g*-MA blend, the interactions with the toughening agent predominate over its plasticizing action.

The evaluation of the interactions extent between reinforcement and a polymer matrix can be achieved from the height at the maximum of the curves giving the variations of  $\tan \delta$  versus temperature and the intensity of  $\tan \delta$  peak is inversely proportional to the interfacial resistance [41, 42]. The decrease in the trPET/SEBS-*g*-MA blend height at the maximum of  $\tan \delta$  with respect to that of vPET/SEBS-*g*-MA blend gives a clear indication that more interactions are involved when trPET is melt mixed with SEBS-*g*-MA.

#### *Thermal Stability of vPET, trPET and Their Mixtures with SEBS-*g*-MA*

Figure 12 shows that, as expected, vPET presents a better thermal stability than trPET. It begins to decompose after 6 min and exhibits a weight loss of approximately 0.01%. The tested sample mass continues to decrease monotonously to attain a weight loss of 0.46% after 30 minutes. However, trPET starts to lose weight after only two minutes of processing, where its weight loss is of about 0.03%, due to the beginning (onset) of several degradation processes such as chains scission and thermal oxidation. The trPET weight loss persists along the test period and attains finally a value of 0.71%. The thermal decomposition of the toughening agent begins gently and later after approximately 8 min then keeps on severely after 10 minutes of processing. After 30 min, the weight loss reaches 3.03%.

After the modification of the resins by the incorporation of 20% of SEBS-*g*-MA to both trPET and vPET, a significant increase in their thermal stability is observed, particularly for the trPET blend. Indeed, the trPET/SEBS-*g*-MA is still thermally stable over a period of 12 min against 15 min for the vPET/SEBS-*g*-MA blend. After 30 min, the two mixtures present a weight loss of about 0.34 and 0.24%, respectively. This important improvement of the recycled resin thermal stability is undoubtedly the result of a strongly reinforced interface promoted by the high trPET concentration of hydroxyl groups and their reaction with the functional groups of the toughening agent.

## CONCLUSIONS

Recycled PET has been submitted to annealing before incorporating a toughening agent which is SEBS-g-MA, in order to improve its performances to enlarge the re-use of the recycled material deriving from the PET wastes and/or get a competing resin that could be a suitable substitute for the virgin resin in several applications. The annealing treatment has been performed to increase the polymer crystallinity, decrease its ability to capture moisture and prevent its hydrolytic degradation during reprocessing. The mechanical, thermal and morphological properties of trPET and its mixtures with SEBS-g-MA have been investigated and compared to those of the vPET ones.

The investigation of the mechanical properties revealed significant improvements of tensile and impact resistances of trPET mixtures with SEBS-g-MA and allowed the achievement of performances that are close or superior to those shown by the virgin resin mixtures. The enhancement of the mechanical performances is favored by the increase in the adhesion of the elastomeric particles to the matrix thanks to the interfacial reaction occurring between the hydroxyl and maleic anhydride groups, as showed by the FTIR analysis. As a result, a good compatibility is attained as evidenced by SEM micrographs.

The dynamic mechanical analysis revealed that the trPET/SEBS-g-MA blend exhibits a higher storage modulus than that obtained for the blend based on the virgin polymer. However, the glass transition temperatures of vPET and trPET matrices revealed small variations due to the competing effects between the plasticizing action exerted by the toughening agent and the interactions intensity at the interface between the recycled polymer and the elastomer.

The benefits of the combination implying annealing followed by reinforcing using the SEBS-g-MA impact modifier are also well perceived on the thermal stability of the crystallized matrix. Indeed, trPET/SEBS-g-MA blend revealed a significant promotion in its thermal stability which that of the virgin resin by permitting a relatively safe processing of the recycled polymer. This reflects a crucial advantage in favor of diminishing PET wastes through encouraging recycled resin re-use and development via mechanical recycling process.

## REFERENCES

1. Y. Zong, Y. Cheng, and G. Dai, *J. Compos. Mater.* **42**, 1571 (2008).
2. Z. Tan, S. Liu, X. Cui, S. Sun, and H. Zhang, *J. Thermoplast. Compos. Mater.* **29**, 833 (2014).
3. S. Deng, Q. Liu, X. Bao, and X. Cai, *Polym.-Plast. Technol. Eng.* **54**, 1184 (2015).
4. M. Raiisi-Nia, A. Aref-Azar, and M. Fasihi, *J. Appl. Polym. Sci.* **131**, 40483 (2014).
5. X. L. Jiang, S. J. Luo, K. Sun, and X. D. Chen, *eXPRESS Polym. Lett.* **1**, 245 (2007).
6. L. Gouisseem, A. Douibi, and D. Benachour, *Polym. Sci., Ser. A* **56**, 844 (2014).
7. H. Inoya, Y. Wei Leong, W. Klinklai, Y. Takai, and H. Hamada, *J. Appl. Polym. Sci.* **124**, 5260 (2012).
8. B. Geyer, G. Lorenzand, and A. Kandelbauer, *eXPRESS Polym. Lett.* **10**, 559 (2016).
9. N. Gamze Karsli, *J. Thermoplast. Compos. Mater.* **30**, 1157 (2015).
10. M. B. Coltelli, S. Bianchi, and M. Aglietto, *Polymer* **48**, 1276 (2007).
11. M. A. Silva Spinace and M. A. De Paoli, *J. Appl. Polym. Sci.* **80**, 20 (2000).
12. N. Torres, J. J. Robin, and B. Boutevin, *J. Appl. Polym. Sci.* **79**, 1816 (2001).
13. Y. Zhang, W. Guo, H. Zhang, and C. Wu, *Polym. Degrad. Stab.* **94**, 1135 (2009).
14. M. Villalobos, A. Awojulu, T. Greeley, G. Turco, and G. Deeter, *Energy* **31**, 3227 (2006).
15. A. A. Tavares, D. F. A. Silva, P. S. Lima, D. L. A. C. S. Andrade, S. M. L. Silva, and E. L. Canedo, *Polym. Test.* **50**, 26 (2016).
16. *Modern Polyesters: Chemistry and Technology of Polyesters and Copolyesters*, Ed. by J. Scheirs and T. E. Long (Wiley, England, 2003).
17. T. Toda, H. Yoshida, and K. Fukunishi, *Polymer* **36**, 699 (1995).
18. N. Chapleau and M. A. Huneault, *J. Appl. Polym. Sci.* **90**, 2919 (2003).
19. J. Su, Y. Li, K. Wang, and Q. Fu, *J. Mater. Sci.* **49**, 1794 (2014).
20. C. Jun, Y. Wei, L. Zhengying, and H. Rui, *J. Mater. Sci.* **39**, 4049 (2004).
21. C. Cazan, M. Cosnita, and A. Duta, *Arabian J. Chem.* **10**, 300 (2015).
22. S. S. Pesetskii, B. Jurkowski, O. V. Filimonov, V. N. Koval, and V. V. Golubovich, *J. Appl. Polym. Sci.* **119**, 225 (2011).
23. Z. Tan, S. Liu, X. Cui, G. Wu, S. Sun, and Huixuan Zhang, *Polym.-Plast. Technol. Eng.* **53**, 141 (2014).
24. S. Paul and D. D. Kale, *J. Appl. Polym. Sci.* **80**, 2593 (2001).
25. Y. Zhang, H. Zhang, L. Ni, Q. Zhou, W. Guo, and C. Wu, *J. Polym. Environ.* **18**, 647 (2010).
26. V. Tanrattanakul, A. Hiltner, E. Baer, W. G. Perkins, F. L. Massey, and A. Moet, *Polymer* **38**, 2191 (1997).
27. W. Loyens and G. Groeninckx, *Polymer* **43**, 5679 (2002).
28. S. Al-Malaika and W. Kong, *Polymer* **46**, 209 (2005).
29. P. Phinyocheep, J. Saelao, and J. Y. Buzaré, *Polymer* **48**, 5702 (2007).
30. M. B. Coltelli, C. Harrats, M. Aglietto, and G. Groeninckx, *Polym. Eng. Sci.* **48**, 1424 (2008).
31. M. B. Coltelli, I. D. Maggiore, S. Savi, M. Aglietto, and F. Ciardelli, *Polym. Degrad. Stab.* **90**, 211 (2005).

32. R. C. Roberts, *J. Polym. Sci., Part B: Polym. Lett.* **8**, 381(1970).
33. D. C. Basset, R. H. Olley, and R. A. H. Al Raheil, *Polymer* **29**, 1745 (1988).
34. E. M. Woo and T. Y. Ko, *J. Colloid Polym. Sci.* **274**, 309 (1996).
35. C. Sawatari and M. Matsuo, *J. Text. Res.* **55**, 547 (1985).
36. C. A. Avila-Orta, J. Francisco, M. Rodriguez, Z. Wang, D. N. Rodriguez, S. H. Benjamin, and F. Yeh, *Polymer* **44**, 1527 (2003).
37. N. K. Kalfoglou, D. S. Skafidas, J. K. Kallitsis, J. C. Lambert, and L. V. Stappen, *Polymer* **36**, 4453 (1995).
38. Z. Z. Yu, M. S. Yang, S. C. Dai, and Y. W. Mai, *J. Appl. Polym. Sci.* **93**, 1462 (2004).
39. S. R. Lim and W. S. Chow, *J. Appl. Polym. Sci.* **123**, 3173 (2012).
40. J. Park, D. Kim, and K. Suh, *J. Appl. Polym. Sci.* **78**, 222 (2000).
41. A. Martinez-Hernandez, C. Velasco-Santos, M. de-Icaza, and V. Castano, *J. Compos.* **38**, 405 (2007).
42. S. Keusch and R. Haessler, *J. Compos.* **30**, 997 (1999).